

THE APACHE POINT OBSERVATORY LUNAR LASER-RANGING OPERATION (APOLLO)

T. W. Murphy, Jr., J. D. Strasburg, C. W. Stubbs, E. G. Adelberger, J. Angle
University of Washington, Dept. of Physics, Box 351560, Seattle, WA 98195

K. Nordtvedt
Northwest Analysis, 118 Sourdough Ridge Road, Bozeman, MT 59715

J. G. Williams, J. O. Dickey
Jet Propulsion Laboratory, California Institute of Technology, Pasadena, CA 91109

B. Gillespie
Apache Point Observatory, PO Box 59, Sunspot, NM 88349-0059

ABSTRACT

Lunar Laser Ranging (LLR) is the only means available for testing Einstein’s Strong Equivalence Principle, on which general relativity rests. LLR also provides the strongest limits to date on variability of the gravitational constant, the best measurement of the de Sitter precession rate, and is relied upon to generate accurate astronomical ephemerides. LLR is poised to take a dramatic step forward, enabled both by detector technology and access to a large-aperture astronomical telescope. Using the 3.5 m telescope at the Apache Point Observatory, we will push LLR into a new regime of multiple photon returns with each pulse, enabling millimeter range precision to be achieved. In order to reap the benefits of this “strong” return, we will incorporate a technologically novel integrated array of avalanche photodiodes—capable of generating a temporal range profile while preserving two-dimensional spatial information. We will also employ a high precision gravimeter at the ranging site to measure local displacements of the earth’s crust to sub-millimeter precision. This approach of obtaining directly relevant measurements relating to the earth surface deformation is to be contrasted with the approach to date that relies strictly on models for this information.

1 Introduction & Scientific Motivation

Lunar Laser Ranging (LLR) has a distinguished history [1, 2] dating back to the placement of retroreflector arrays on the lunar surface by the Apollo 11 astronauts. Additional reflectors were left by the Apollo 14 and Apollo 15 astronauts, and two French-built reflector arrays were placed on the Moon by the Soviet Luna 17 and Luna 21 missions. Early range precisions hovered around 25 cm from 1970–1975, followed by a period of 12–16 cm precision until 1984, after which the McDonald Laser Ranging system (MLRS) drove the precision into the 3 cm regime in the mid-to-late 1980s. MLRS has continued to deliver 2–3 cm lunar range data to the present, and was joined in the early 1990s by a French LLR system at the Observatoire de la Côte d’Azur (OCA) with comparable range precision.

The LLR measurements of the past have contributed to a wide range of scientific investigations [3, 4, 5], are today solely responsible for production of the lunar ephemeris, and dominate the determination of earth orientation and precession [6]. On the fundamental scientific front, LLR provides the *only* means for testing Einstein’s Strong Equivalence Principle (SEP)—the statement that *all* forms of mass and energy have equivalent quantities of inertial and gravitational mass. The SEP is more restrictive than the weak EP, which applies to non-gravitational mass-energy—effectively probing the compositional dependence of gravitational acceleration. It is the equivalence principle which leads to identical accelerations of compositionally different objects in the same gravitational field, and also allows gravity to be viewed as a geometrical property of spacetime—leading to the general relativistic interpretation of gravitation. In addition to the SEP, LLR is capable of measuring the time variation of Newton’s gravitational constant, G , providing the strongest limit available for the variability of this “constant”. LLR can also precisely measure the de Sitter precession—effectively a spin-orbit coupling affecting the lunar orbit in the rotating earth reference frame. The interior, tidal response, and physical librations (rocking) of the moon are all probed by LLR, making it a valuable tool for physical selenography.

We have initiated a project appropriately dubbed APOLLO (Apache Point Lunar Laser-ranging Operation) that will push LLR into the regime of millimetric range precision. Primarily interested in fundamental physics, we will ultimately be able to translate the increased range precision into an order-of-magnitude improvement in the determination of fundamental physics parameters. Specifically, assuming improvements of a factor of ten over current measurements [3, 5], we will test:

- the Weak Equivalence Principle to a part in 10^{14} ,
- the Strong Equivalence Principle to a few parts in 10^5 ,
- de Sitter precession to a few parts in 10^4 , and
- the time variation of G to a part in 10^{13} per year.

This last number is impressive considering that the expansion rate of the universe is approximately one part in 10^{10} per year, so that if the gravitational constant scaled with the size of the universe, it too would change at this rate.

As an illustration of how a SEP violation would appear in the lunar range data, consider that the earth’s gravitational self-energy—amounting to $m_E/M_\oplus = E/M_\oplus c^2 = 4.6 \times 10^{-10}$ of the earth’s total mass—does not obey the equivalence principle. In other words, it does not have equivalent values of inertial and gravitational mass, and therefore does not accelerate towards the sun at the same rate as the normal matter comprising the earth and the moon. Let us further assume the case of maximal violation wherein, for example, the earth’s self-energy has the expected amount of gravitational mass, but no inertial mass. The net effect would be an additional acceleration of the earth *towards* the sun not experienced by the moon with its negligible gravitational self-energy. From our perspective on earth, this would appear as a displacement, or polarization, of the lunar orbit *away* from the sun with an amplitude of 13 m. If the violation went the other way, with the self energy possessing inertial mass but not gravitational mass, the lunar orbit would appear to be polarized towards the sun by the same amplitude. The calculation of the amplitude is complicated [7, 8, 9], but a crude estimate may be derived by multiplying the earth’s orbital radius of 1.5×10^{11} m by the 5×10^{-10} contribution to the earth’s mass from the self-energy to yield 75 m.

It is already known via LLR that the moon’s orbit is *not* displaced by a violation of the SEP at the ~ 5 mm level of precision—based on 2–3 cm raw range precisions—constraining the SEP violation at the level of about 5 parts in 10^4 . The high quality data from APOLLO should permit

sub-millimeter determinations of the SEP-induced polarization of the lunar orbit, thereby achieving a few parts in 10^5 precision on the potential SEP violation. Various alternative theories of physics (string, or M-theory, for example) predict new particles such as the dilaton and moduli that couple with gravitational strength and whose exchange violates the SEP.

2 The Photon Premium

The APOLLO system, like other laser ranging systems, is based on measuring the time-of-flight of a short-pulse laser reflected off a distant target—in this case the retroreflector arrays on the lunar surface. One-millimeter range determination corresponds to a mere 6 ps of round-trip travel time. Recognizing that the moon undergoes apparent librations—orientation variations due to a constant rotation rate but an elliptical, inclined orbit—of up to 10° in magnitude, one quickly sees that the passive array of retroreflectors spans a finite, measurable range of distances from the transmit point. The $0.6 \times 1.0 \text{ m}^2$ Apollo 15 array, for instance, will in the worst case have a corner-to-corner range spread of $\approx 1.2 \tan 10^\circ \text{ m}$, or 210 mm, translating to 1.4 ns of round-trip time. The root-mean-square (RMS) range spread becomes about 400 ps, worst case. To determine the centroid of this range spread to 1 mm precision, or 7 ps, one must collect at least $(400/7)^2 \approx 3,000$ photons. For reference, the current 2 cm RMS range precision requires only about 10 photons at the worst-case orientation of the retroreflector array.

Clearly, high precision LLR will require high photon return rates. An order-of-magnitude improvement in range demands a two orders-of-magnitude gain in photon number—at least to the extent that one is dominated by statistical errors. The currently operating LLR stations in Texas (McDonald Laser Ranging System—MLRS—[10]) and France (Observatoire de la Côte d’Azur—OCA—[11]) typically receive 0.01 photons per pulse during normal operation. A typical “normal point” is constructed from 5–100 return photons, spanning 10–45 minutes of observation [2]. We expect APOLLO to detect 5–10 photons with every pulse, or about 100 photons per second. At this return rate, we will achieve the necessary photon number for millimeter precision on the timescale of one minute. The key to this success is access to a large aperture telescope at an observing site with excellent atmospheric seeing.

The expected return photon rate is dominated by the signal loss from divergence of the outgoing and return beams. The outgoing beam, even if perfectly collimated, is limited by the atmosphere to a divergence of one to a few arcseconds. At one arcsecond, the beam size on reaching the lunar surface is about 2 km in diameter. The small corner cubes comprising the Apollo arrays are 3.8 cm in diameter, and because they are not diffraction limited devices, and are additionally susceptible to thermal deformations, the effective beam from the retroreflectors spans 7–10 arcsec [2], or about 18 km on the earth’s surface. If Φ is the atmospheric divergence, ϕ the corner-cube divergence, D the diameter of the collecting telescope, and d the diameter of the n corner cubes in the array, then the link efficiency is

$$\epsilon = \eta^2 f Q \left(\frac{nd^2}{r^2 \Phi^2} \right) \left(\frac{D^2}{r^2 \phi^2} \right).$$

Here, r is the distance to the moon, η is the telescope/atmospheric transmission efficiency (experienced both ways), f is the receiver throughput—dominated by a narrow-band filter, and Q is the detector efficiency. With 1 arcsec seeing, 40% telescope efficiency, 25% receiver efficiency, and 30% detector quantum efficiency, the APOLLO link efficiency (to the smaller Apollo arrays) is a staggeringly small 1.7×10^{-17} . However, a 115 mJ laser pulse at 532 nm contains 3.1×10^{17} photons, placing us squarely into the 5–10 photon-per-pulse detection regime. Speckle interference

of the beam pattern on the moon will make the photon return rate highly variable, with 50% of pulses returning between 1–10 detected photons (based on an average of six).

3 APOLLO System Overview

The APOLLO apparatus will be located at the Apache Point Observatory (APO) in southern New Mexico, on a 2,880 m (9,200 ft) ridge overlooking the White Sands Missile Range. The 3.5 m telescope is run by a consortium of universities, with the University of Washington acting as the controlling agency, with 30% of the telescope time. Our access to the APO telescope places us in a unique position to perform a fundamental physics experiment using a first-class astronomical facility. The gain APO offers over existing LLR operations is substantial. Compared to MLRS, the telescope has a factor of 20 greater light-collecting area, but more importantly, the APO site-plus-telescope routinely delivers one arcsecond and better image quality, compared to the ~ 5 arcseconds typical for MLRS. The improvement in seeing, or atmospheric blurring, cannot be overstated; it gives both increased laser beam intensity on the moon and reduces the lunar background admitted through a well-matched spatial filter on the receiver. Each of these effects is proportional to the inverse square of the seeing, so that the signal-to-noise ratio of the lunar return is inversely proportional to the fourth power of the point-source image size. Thus APOLLO stands to gain a factor of $20 \times 25 = 500$ in return signal strength over MLRS, and additional factor of 25 in signal-to-noise (through background reduction). Similar analysis suggests that APOLLO will gain a factor of 50 in signal over the OCA LLR facility, with its 1.5 m telescope and perhaps 3 arcsec seeing.

The greater return rate of APOLLO will, in addition to improving the statistical error, also allow us to investigate many possible systematic effects that could not be addressed previously. For example, APOLLO will be able to work in high-background environments—largely due to the small spatial apertures (~ 0.3 arcsec) of the array detector elements (discussed below). Operation during full moon and even daylight will not interfere with the high signal-to-noise quality of the APOLLO data. Because of the difficulties of ranging in high background conditions, most lunar ranges have been obtained near the quarter-moon phase where target acquisition is easier and background is not as severe. Unfortunately, the EP signal, which corresponds to a displacement of the lunar orbit towards or away from the sun, passes through a *null* at quarter moon. Uniform phase coverage of lunar ranges alone could improve the SEP determination by better isolating the interesting scientific signals from aliasing or biases due to any unmodeled or mismodeled signals [12]. Aside from about 2.5 days on either side of new moon, APOLLO will be able to fully sample the lunar cycle. The high count rate capability of APOLLO will also allow us to measure routinely the total laser/timing system response function as well as the lunar retroreflector array “profile”—all based on the temporal distribution of the multiple photon returns within individual pulses. Asymmetries in these profiles would lead to systematic range offsets if one simply relied on centroids to determine the range information.

3.1 APOLLO Laser

APOLLO will utilize an off-the-shelf Q-switched, mode-locked Nd:YAG laser operating at a wavelength of 532 nm [13]. This laser has a pulse-width of 120 ps FWHM (full-width at half-max), a pulse energy of 115 mJ, and a repetition rate of 20 Hz. Though our ultimate goal is 6 ps timing precision, as noted before, the libration effect on the retroreflector arrays spreads the return pulse to widths typically around 300 ps, and potentially exceeding 1 ns. There is no benefit, then, in demanding a laser pulse width less than ~ 100 ps. The laser will be expanded to fill the 3.5 m

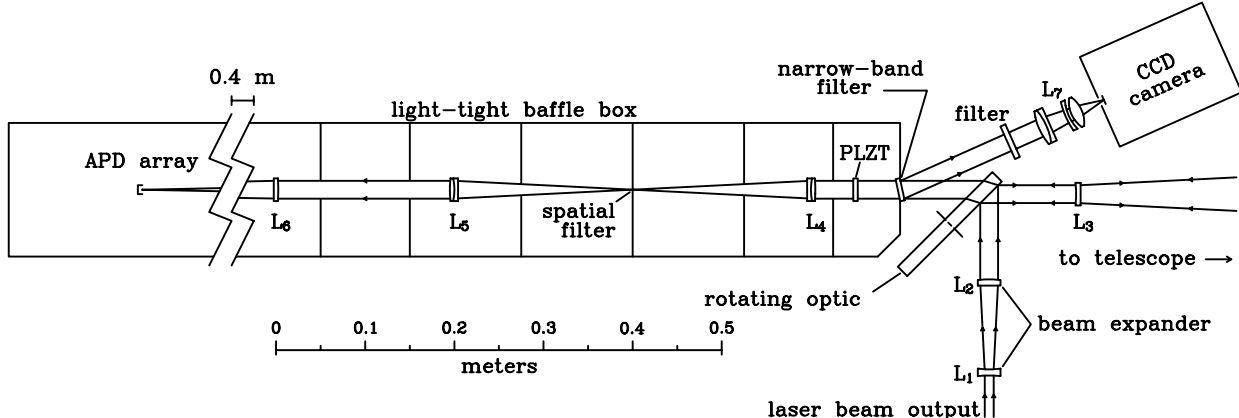


Figure 1: The APOLLO optical layout, minus laser and telescope. The $f/10$ beam to the telescope is shared by the transmit and receive paths, with a rotating optic switching between the two.

aperture of the APO telescope. In this way, the very high peak power (in the GW range) does not harm the telescope mirror coatings, and presents less of an eye hazard to curious pilots.

3.2 APOLLO Optics

The optical system for APOLLO, shown in Fig. 1, consists of transmit and receive paths, both sharing the same path through the telescope. A negative lens collimates light from the telescope, or alternatively, expands the collimated laser beam to fill the telescope aperture. The switch between the two paths is explained in section 3.4. The transmit path includes a variable beam expander, and otherwise consists of simple steering mirrors. The receive path, with its photon-sensitive detector at a reimaged focal plane, will be carefully protected from stray laser light. The transmit/receive switch provides most of the protection, and baffling plus spatial filtering helps eliminate remaining light. A ~ 0.5 nm bandpass filter at the entrance to the receiver prevents the bulk of the high background photons from the moon or daylight sky from entering the baffled enclosure. The rejected light can be used to feed an off-band CCD imager for purposes of acquisition and tracking.

3.3 APD Arrays

Perhaps the most technologically advanced component of the APOLLO apparatus is the integrated array of avalanche photodiodes (APDs) we will use as our detector. We adopt this technology to deal with multiple photon returns within each pulse. Because the photons are clustered within one nanosecond, a single-photon detector would record the arrival time of only the *first photon* in the pulse. However the important quantity is the *centroid* of the return packet (assuming symmetric pulse distribution), so that we must record the arrival times of each photon in the pulse.

Avalanche photodiodes have long been used as single-photon detectors, operating beyond their breakdown voltage in “Geiger mode”. Detectors a few tens of microns thick achieve visible photon detection efficiencies in excess of 60%, time resolution in the tens of picoseconds, and have breakdown voltages around 20–40 V [14].

MIT Lincoln Labs has recently begun exploring integrated APD arrays, with elements arranged in square patterns with $100 \mu\text{m}$ spacing. The Lincoln Labs designs feature active area diameters ranging from 20–40 μm , with breakdown voltages around 25 V, and photon detection efficiencies

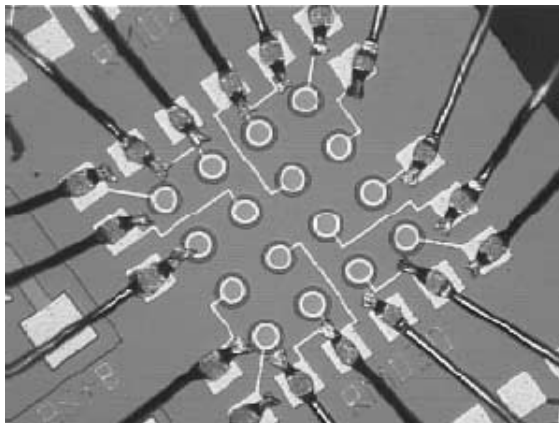


Figure 2: The 4×4 APD array from Lincoln Labs. The individual elements are the circular pads $30 \mu\text{m}$ in diameter, separated by $100 \mu\text{m}$ in each dimension. We may ultimately employ a much larger array in APOLLO. We are currently testing the pictured array, characterizing its time response and detection efficiency.

upward of 50%. We plan to use one of these arrays at the focal plane of our LLR receiver, in such a way as to oversample the point-spread-function across a handful of elements (e.g., via 0.3 arcsec pixels). A lenslet array in front of the detector recovers a nearly 100% fill-factor, compared to the 3–12% fill-factors of the arrays as fabricated. An oversampled APD array provides a variety of advantages:

- The multi-photon return is spread across many detector elements, so that individual elements are statistically unlikely to detect more than one photon in a given pulse. As a consequence, one obtains a range “profile” of the reflector array with each shot.
- Two-dimensional spatial information is preserved so that the position of the return pulse is known, and real-time guiding corrections can be based on this information.
- Systematics such as beam focus, transmit/receive co-alignment, etc. may be evaluated based on the 2-D footprint of the return (both from the lunar target and a calibration corner cube internal to the telescope enclosure).

We plan to modulate the APD bias voltage in such a way that the APD is “gated on” only for short intervals ($\sim 100 \text{ ns}$) around the expected pulse return time.

We are currently working with two 4×4 prototype APD arrays via an active collaboration with Lincoln Labs, and plan to eventually work with a format as large as perhaps 10×10 (LL has fabricated 32×32 devices). The optical design allows for easy upgrades as larger format detectors become available. Figure 2 shows the appearance of one of the 4×4 arrays currently in hand.

3.4 Calibration & Beam Switching

Filling the entire 3.5 m aperture with the outgoing laser beam demands the ability to switch between transmit and receive modes. This will be accomplished via a rotating optic—mostly transmissive and anti-reflection coated for passing the return photons, but with a small dielectric patch for laser reflection. The spinning optic will be controlled via a stepper motor, and the laser slaved to the motor so that the reflective patch always intercepts the outgoing beam, directing it towards the

telescope. The motor rate can be varied slightly around 20 Hz in such a way as to guarantee that the lunar return photons arrive nearly 180° out of phase from the outgoing pulse. A small corner cube placed at the telescope exit aperture will redirect a tiny fraction of the outgoing beam back toward the transmitter/receiver. The photons returning from this retroreflector will calibrate the departure time of the pulse. The position of the corner cube will be mechanically referenced to the intersection of the telescope axes, which is the stationary positional reference for the LLR station. A technical challenge exists in that a 1 cm diameter corner cube will intercept some 2×10^{12} photons per pulse, with potentially 10^{11} photons capable of being detected. This must be attenuated by about 10^{10} for the APD array to detect a number of photons comparable to that from the lunar return. The attenuation is handled through a combination of crossed polarizers in front of the calibration corner cube, and reflective and optically dense coatings on the rotating optic. This general calibration technique is shared by other laser ranging systems, though the advantages of multiple photon capability again become apparent in that *each pulse* gets calibrated. Single-photon ranging systems must prevent a high photon rate from biasing the calibration to early times, so that typically only one out of every 5–10 pulses gets calibrated.

In addition to providing calibration to a fixed spatial reference (the telescope axis intersection), the photons from the calibration corner cube enable a characterization of the convolution of time responses of the detector, the timing electronics, and the laser pulse shape. Detailed knowledge of this total effective profile will be invaluable in interpreting the temporal profile returning from the moon.

3.5 APOLLO Timing System

The timing scheme for APOLLO is based on a GPS-slaved clock [15] providing a highly stable 100 MHz frequency reference, operated in conjunction with commercial 12-bit time-to-digital converters (TDCs) having 25 ps resolution [16]. The TDCs keep track of the precise time interval between APD detection events and the next clock pulse, while a digital counter system continuously keeps track of the number of clock pulses between events in a redundant way. The GPS-slaved clock also provides a reference to Coordinated Universal Time (UTC) with a typical error of less than 40 ns. For reference, the range between the moon and our station on the earth’s surface changes by as much as 400 m s^{-1} , mostly due to earth rotation, meaning that millimeter range precision demands knowledge of absolute time only at the few microsecond level. All multiplexing associated with the multiple APD elements is handled in the APD array itself and the TDCs, which come in 16-plex units. All other timing control is independent of the number of channels employed, and consists of a system of counters, comparators and latches, nearly all of which can be accommodated on a single Programmable Array Logic (PAL) chip. The timing system will also control the APD gating action, with the 100 MHz clock signal enabling 10 ns resolution in gate placement and duration.

The signal from the calibration corner cube allows for a differential measurement between the departure time of the outgoing beam and the corresponding lunar return approximately 2.5 s later. A fast photodiode within the laser performs the dual function of triggering the timing control system when the laser fires, and providing a high signal-to-noise determination of the laser start time, to be referenced to the APD detection time of the few-photons returning from the calibration corner cube.

The expected statistical RMS timing errors are shown in Table 1. The range given for the retroreflector spread represents typical values, assuming a lunar libration angle between $5\text{--}8^\circ$, and a reflector spanning 0.5–0.8 m. The retroreflector array generally dominates the error budget, so that ~ 1000 photons are typically required to achieve 1 mm statistical error.

Statistical Error Source	RMS Error (ps)	One-way Error (mm)
Laser Pulse (115 ps FWHM)	50	7.5
APD jitter	50	7.5
TDC jitter	25	3.8
100 MHz Freq. Reference	< 10	< 1.5
APOLLO System Total	75	11
Lunar Retroreflector Array	80–230	12–35
Grand Total	110–240	16–36

Table 1: Single-photon random error budget

3.6 Supplemental Metrology

The primary APOLLO system measures the time delay of photons making a round-trip from our telescope to the lunar surface and back. We ultimately want to convert this to a distance from the center-of-mass of the earth to the center-of-mass of the moon. To do this, one must understand the body rotations and the positional displacements of the surface sites with respect to the center-of-masses of the respective bodies. If the earth and moon were perfectly rigid bodies, this would reduce to a problem of orientation and constant offsets. But reality is, of course, not that kind. The earth and moon have fluid interiors allowing flexure in the presence of tidal forces. The moon, being locked in tidal resonance with the earth, experiences relatively small fluctuations of its surface, in the neighborhood of 10 cm. The earth’s crust, however, rotating under the tidal potential, oscillates with a peak-to-peak amplitude of approximately 0.35 m every 12 hours. Worse than the predictable tidal oscillations is the fact that the earth has weather—something the moon does not have to contend with. A variety of meteorologically-related phenomena can act to load local regions of the crust, depressing the crust by some number of millimeters under the load. These include loadings from atmosphere (high pressure systems), ocean (water piled up on regional coast), and ground water (e.g., after a big rain). An additional effect comes from the path delay through the atmosphere due to its non-unity refractive index. From the APO site, the one-way atmospheric zenith delay amounts to about 1.6 m of effective range.

Traditionally, these effects—which are common to LLR and the more ubiquitous satellite laser ranging (SLR)—have been combated through a combination of metrology and modeling. Typically, the ranging station measures local temperature, pressure, and relative humidity at the surface. This allows one to model the atmospheric delay, which is dominated by the pressure measurement alone. Early models had uncertainties in the 5–10 mm range for reasonable elevation angles [17], though more recent efforts have produced a model claiming 3 mm accuracy down to 10° above the horizon, and sub-millimeter performance above 20–30° elevation [18]. Atmospheric loading relies on a model using station pressure and average pressure within a 1000 km radius as inputs. Ocean loading has been handled strictly in the modeling domain, and ground water has been largely ignored.

In addition to measuring local atmospheric conditions, APOLLO will incorporate a precision gravimeter [19] at the site, capable of sensing vertical displacements as small as 0.1 mm simply on account of the altered distance to the center of the earth and the corresponding change in the gravitational field. A continuous record of local gravimetry would be sensitive to not only the rich spectrum of tidal displacements, but will also record loading of various forms. This statement is a gross simplification, in the sense that the gravimeter is directly sensitive to the gravitational tug of atmosphere and ground water. Thus, for instance, while high atmospheric pressure pushes down on the earth’s crust—increasing local gravity—it also attracts the gravimeter test mass upward, thereby reducing the perceived gravity. In fact, in this case, the direct attraction wins, and high

pressure results in a lower value of local gravity. Conversely, ground water increases local gravity both through crustal displacement and via direct gravitational attraction.

Though the gravimeter susceptibilities prevent it from independently providing an accurate characterization of crustal motion, the following general statements can be made in favor of including such a device in the APOLLO system.

- If concentrating on the Equivalence Principle signal, with a well defined period of 29.53 days, meteorological effects average away, and only the tidal response (and associated ocean-loading terms) carries power at the SEP signal frequency. The gravimeter *will* reliably measure the amplitude and phase of the tidal motions with the synodic frequency, and is therefore a valuable tool in the measurement of the SEP. Long-term gravimetry records indicate that the ~ 8 mm monthly tidal amplitude can be determined at the level of a few tenths of a millimeter [20, 21].
- Improved modeling is driven by improved measurement. By placing a device that will provide a gravity measurement at the site, we simply cannot go wrong in ultimately realizing better models for the crustal displacement at the site. This *must* be better than blind reliance on models to describe the motions of the local crust.

4 Conclusions

The APOLLO effort is an exciting new leap into the field of gravitational physics through lunar ranging. Access to a large telescope and inclusion of new, capable technologies promise to push the measurement accuracy of the lunar range into the millimeter regime, leading to the most precise measurements available of the SEP, rate of change of G , and de Sitter precession.

We acknowledge a grant from the microgravity division of NASA, for which our primary tasks include: thorough analysis of modeling capabilities and identification of sources of systematic error, characterization and deployment of APD array technology, and a study of the feasibility of performing LLR from a space platform. This last effort stems from the realization that meteorology plays an important role in ground-based LLR, and that ultimately one would like to be divorced from the intricate details of the earth's crustal response, obtaining a range more representative of the earth-moon center-of-mass separation.

References

- [1] Bender, P. L., Currie, D. G., Dicke, R. H., Eckhardt, D. H., Faller, J. E., Kaula, W. M., Mullholland, J. D., Plotkin, H. H., Poultney, S. K., Silverberg, E. C., Wilkinson, D. T., Williams, J. G., & Alley, C. O., "The Lunar Laser Ranging Experiment", *Science*, **182**, 229, (1973)
- [2] Dickey, J. O., Bender, P. L., Faller, J.E., Newhall, X. X., Ricklefs, R. L., Ries, J. G., Shelus, P. J., Veillet, C., Whipple, A. L., Wiant, J. R., Williams, J. G., & Yoder, C. F., "Lunar Laser Ranging: A Continuing Legacy of the Apollo Program", *Science*, **265**, 482, (1994)
- [3] Williams, J. G., Newhall, X. X., & Dickey, J. O., "Relativity parameters determined from lunar laser ranging", *Physical Review D*, **53**, 6730, (1996)

- [4] Baeßler, S., Heckel, B. R., Adelberger, E. G., Gundlach, J. H., Schmidt, U., & Swanson, H. E., “Improved Test of the Equivalence Principle for Gravitational Self-Energy”, *Physical Review Letters*, **83**, 3585, (1999)
- [5] Anderson, J. D., & Williams, J. G., “Long-Range Tests of the Equivalence Principle”, *Classical and Quantum Gravity*, **18**, 2447, (2001)
- [6] Standish, E. M., Newhall, X. X., Williams, J. G., & Folkner, W. M., “JPL Planetary and Lunar Ephemerides, DE403/LE403”, *JPL IOM* 314.10 – 127, (1995)
- [7] Nordtvedt, K., “The Relativistic Orbit Observables in Lunar Laser Ranging”, *Icarus*, **114**, 51, (1995)
- [8] Damour, T., & Vokrouhlický, D., “Equivalence Principle and the Moon”, *Physical Review D*, **53**, 4177, (1996)
- [9] Müller, J., & Nordtvedt, K., “Lunar laser ranging and the equivalence principle signal”, *Physical Review D*, **58**, 200, (1998)
- [10] <http://almagest.as.utexas.edu/~rlr/mlrs.html>
- [11] Samain, E., et al., *Astron. & Astrophys. Suppl. Ser.*, **130**, 235, (1998)
- [12] Nordtvedt, K., “Optimizing the observation schedule for tests of gravity in lunar laser ranging and similar experiments”, *Classical Quantum Gravity*, **15**, 3363, (1998)
- [13] <http://www.psplc.com/leopard.html>
- [14] Cova, S., Ghioni, M., Lacaíta, A., Samori, C., & Zappa, F., “Avalanche photodiodes and quencing circuits for single-photon detection”, *Applied Optics*, **35**, 1956, (1996)
- [15] <http://www.truetime.com/indexP.html>
- [16] <http://www.phillipsscscientific.com/phisci1.htm>
- [17] Marini, J. W., & Murray, C. W., Jr., “Correction of Laser Range Tracking Data for Atmospheric Refraction at Elevation Angles Above 10 Degrees”, *NASA Technical Report*, X-591-73-351, (1973)
- [18] Pavlis, E. C., & Mendes, V. B., “Improved Mapping Functions for Atmospheric Refraction Corrections for LR: Preliminary Validation Results”, 12th International Workshop on Laser Ranging, Matera, Italy, (2000)
- [19] http://www.gwrinstruments.com/GWR_tidalbro.html
- [20] Boy, J.-P., Hinderer, J., Gegot, P., “Global Atmospheric Loading & Gravity,” *Phys. of Earth & Planetary Inter.*, **109**, 161, (1998)
- [21] Goodkind, J. M., “Test of theoretical solid earth and ocean gravity tides”, *Geophysics Journal International*, **125**, 106, (1996)